ISSN 1990-7931, Russian Journal of Physical Chemistry B, 2016, Vol. 10, No. 5, pp. 801–809. © Pleiades Publishing, Ltd., 2016.
Original Russian Text © V.Ya. Basevich, A.A. Belyaev, S.N. Medvedev, V.S. Posvyanskii, F.S. Frolov, S.M. Frolov, 2016, published in Khimicheskaya Fizika, 2016, Vol. 35, No. 10, pp. 32–41.

COMBUSTION, EXPLOSION, AND SHOCK WAVES

A Detailed Kinetic Mechanism of Multistage Oxidation and Combustion of Isooctane

V. Ya. Basevich[a, b], A. A. Belyaev[a, b], S. N. Medvedev[a, b], V. S. Posvyanskii[a], F. S. Frolov[a, b], and S. M. Frolov[a, b, c, *]

[a] *Semenov Institute of Chemical Physics, Russian Academy of Sciences, Moscow, Russia*
[b] *Center of Pulse Detonation Combustion, Moscow, Russia*
[c] *National Research Nuclear University Moscow Engineering Physics Institute, Moscow, Russia*
**e-mail: smfrol@chph.ras.ru*

Received October 23, 2015

Abstract—This study has been focused on the construction of a detailed kinetic mechanism of oxidation and combustion of isooctane (2,2,4-trimethylpentane) to describe both high-temperature reactions and the low-temperature multistage process with separated stages of "cool" and "blue" flames and hot explosion. In accordance with the proposed mechanism, isobaric autoignition, compression-induced autoignition, and flame propagation characteristics have been calculated; the calculation results have been compared with the experimental data. Satisfactory qualitative and quantitative agreement of the calculation and experimental results has been obtained.

Keywords: alkanes, isooctane, kinetic mechanisms, autoignition, multistage pattern, flame propagation, droplet combustion

DOI: 10.1134/S199079311605016X

INTRODUCTION

On the basis of generalization of a large body of experimental data, the concept of a multistage autoignition of hydrocarbons with separated stages of "cool" and "blue" flames and hot explosion has been introduced [1]. A multistage pattern is observed in many experiments on the oxidation of hydrocarbons, particularly isooctane (i-C_8H_{18}) [1]. In addition, a separate region of blue flame located outside the autoignition boundaries was observed for isooctane [2]. Detailed kinetic mechanisms (DKMs) of oxidation and combustion of isooctane have been already proposed in the literature (see, e.g., [3, 4] and later reports). However, none of these studies has proved that these DKMs adequately describe the multistage autoignition of isooctane with the three above stages. An exception is probably provided by [5]. The authors of that study, which addresses the phenomenology of autoignition of reference fuels, refer to blue flame as "preignition" and give a complex kinetic explanation to it (via reactions with aromatic structures), which cannot be applied to individual normal hydrocarbons and their isomers.

Previously, we have offered a kinetic explanation for the occurrence of blue flame in the case of normal alkanes including cetane [6], isobutane [7], isopentane (2-methylbutane), and isohexane (2-methylpentane) [8]. The aim of this study is to construct a DKM of oxidation and combustion of isooctane (2,2,4-trimethylpentane) to describe not only the high-temperature, but also low-temperature reactions of multistage oxidation and combustion as adequately as reasonably possible.

CONSTRUCTION OF THE MECHANISM

The phenomenology of oxidation and combustion of hydrocarbons is known to exhibit great generality [1]. The DKM of multistage oxidation and combustion of i-C_8H_{18} was constructed on the basis of a nonextensive approach using the analogy technique [6–8]. The nonextensive approach assumes that low-temperature branching is associated with a group of reactions with a single addition of an oxygen atom (to the linear portion of the molecule) and the number of additional components limited to one of each of the main isomerized components that corresponds to each normal-structure component and represents the entire group of species of different structure, yet with a given gross formula (the oxidation pathway involving it is assumed to be the most probable). The analogy technique is used to select reactions that are important for the description of a multistage pattern; it has proved itself in the study of the above normal alkanes and their isomers.

To construct a new mechanism, nine isomerized derivatives of two hydrocarbons—isoheptane (2,2-dimethylpentane $CH_3C(CH_3)_2C_3H_7$) and isooctane (2,2,4-tri-

New reagents of the mechanism of oxidation and combustion

No.	Component	Formula
1.	Hydrocarbon 2,2-dimethylpentane	$CH_3C(CH_3)_2C_3H_7$
2.	Hydrocarbon radical	$CH_3C(CH_3)_2C_3H_6$
3.	Peroxy radical	$CH_3C(CH_3)_2C_3H_6O_2$
4.	Hydroperoxide	$CH_3C(CH_3)_2C_3H_6O_2H$
5.	Oxyradical	$CH_3C(CH_3)_2C_3H_6O$
6.	Aldehyde	$CH_3C(CH_3)_2C_2H_4CHO$
7.	Aldehyde radical	$CH_3C(CH_3)_2C_2H_4CO$
8.	Unsaturated hydrocarbon	$CH_3C(CH_3)_2C_3H_5$
9.	Unsaturated hydrocarbon radical	$CH_3C(CH_3)_2C_3H_4$
10.	Hydrocarbon 2,2,4-trimethylpentane	$CH_3C(CH_3)_2CH_2CH(CH_3)CH_3$
11.	Hydrocarbon radical	$CH_3C(CH_3)_2CH_2CH(CH_3)CH_2$
12.	Peroxy radical	$CH_3C(CH_3)_2CH_2CH(CH_3)CH_2O_2$
13.	Hydroperoxide	$CH_3C(CH_3)_2CH_2CH(CH_3)CH_2O_2H$
14.	Oxyradical	$CH_3C(CH_3)_2CH_2CH(CH_3)CH_2O$
15.	Aldehyde	$CH_3C(CH_3)_2CH_2CH(CH_3)CHO$
16.	Aldehyde radical	$CH_3C(CH_3)_2CH_2CH(CH_3)CO$
17.	Unsaturated hydrocarbon	$CH_3C(CH_3)_2CH_2C(CH_3)CH_2$
18.	Unsaturated hydrocarbon radical	$CH_3C(CH_3)_2CH_2C(CH_3)CH$

methylpentane $CH_3C(CH_3)_2CH_2CH(CH_3)CH_3$)—were added to each of the components of DKM of oxidation and combustion of normal alkane—*n*-octane C_8H_{18}—and isomerized alkanes—isobutane (2-methylpropane $(CH_3)C(CH_3)HCH_3$), isopentane (2-methylbutane $(CH_3)CH(CH_3)C_2H_5$), and isohexane (2-methylpentane $(CH_3)CH(CH_3)C_3H_7$) [8] (see the table); their reactions with each other and other DKM components were also added. It was assumed that, in a large number of various reactions, the leading role is played by reactions that occur via reducing the number of attached methyl groups—deisomerization reactions—to form intermediate stable isomerised hydrocarbon molecules of 2,2-dimethylpentane $CH_3C(CH_3)_2C_3H_7$, 2-methylpentane $CH_3CH(CH_3)C_3H_7$, 2-methylbutane $CH_3CH(CH_3)C_2H_5$, and 2-methylpropane $CH_3CH(CH_3)CH_3$ and respective normal hydrocarbons including methane. Under this assumption, all the other elementary events that increase the "linear" five-membered portion of the isooctane molecule (carbon chain) do not affect the oxidation rate of isooctane. The resulting DKM includes 763 reactions involving normal-structure components and 987 reactions involving isomerized components. The total number of components involved in the mechanism composed of 1750 reactions is 144.

The thermochemical parameters of the components, i.e., enthalpy ΔH°_{f298}, entropy S°_{298}, and coefficients c_0, c_1, c_2, c_3, and c_4 in the formula of specific heat at a constant pressure $c_p = c_0 + c_1T/10^3 + c_2T^2/10^6 + c_3T^3/10^9 + c_4T^4/10^{12}$ for low- and high-temperature ranges were calculated on the basis of the known recommendations and additivity rules [9].

The selection of the Arrhenius parameters of rate constants of many reactions in the developed DKM is hindered by the lack of experimental data. Therefore, the kinetic parameters were calculated as described in [7] on the basis of an array of reaction constants of the normal-structure components using a two-parameter form of the rate constant of an elementary event with preexponential factor A and activation energy E:

$$A_{i(i)} = A_{i(n)} \exp[(\Delta S_{i(i)} - \Delta S_{i(n)})/R],$$
$$E_{i(i)} = E_{i(n)} - 0.25[\Delta H_{i(i)} - \Delta H_{i(n)}]$$

for exothermic reactions and

$$E_{i(i)} = E_{i(n)} + 0.75[\Delta H_{i(i)} - \Delta H_{i(n)}]$$

for endothermic reactions, where $A_{i(i)}$ and $E_{i(i)}$ are the preexponential factor and the activation energy in the expression for the rate of the ith reaction involving isomerized components (i), $\Delta S_{i(i)}$ and $\Delta S_{i(n)}$ are the respective entropy changes in the ith reaction, $A_{i(n)}$ and $E_{i(n)}$ are the preexponential factor and the activation energy in the expression for the rate of the ith reaction involving only normal-structure components (n), $\Delta H_{i(i)}$ and $\Delta H_{i(n)}$ are the respective enthalpy changes in the ith reaction, T is the temperature, and R is the gas constant.

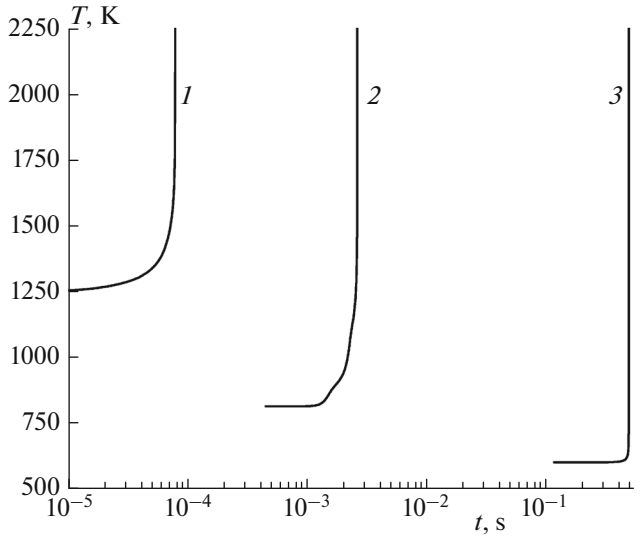

Fig. 1. Calculated temperature–time dependences during the autoignition of stoichiometric ($f = 1.0$) isooctane–air mixtures at an initial temperature of $T_0 = (1)$ 1250, (2) 813, and (3) 600 K and an initial pressure of $P = 36$ atm.

The resulting Arrhenius parameters were corrected only for a limited number of reactions (less than ten).

VERIFICATION OF THE MECHANISM

Autoignition of Gas Mixtures

The developed DKM was verified by comparing the calculated parameters of autoignition of isooctane with the experimental results. Calculations were conducted using the kinetic program developed by M.G. Neigauz at Semenov Institute of Chemical Physics, Russian Academy of Sciences. The following ranges of initial data were used in the calculations: temperature T_0, 600–1850 K; pressure P, 0.8–36 atm; and mixture composition determined by equivalence ratio f, fuel-lean to fuel-rich; argon and nitrogen were used as a diluent.

Figure 1 shows typical calculated temperature–time dependences in the case of autoignition of stoichiometric isooctane–air mixtures characteristic of high, moderate, and low initial temperatures. At high temperatures (>1000 K), autoignition occurs in a single stage. At moderate temperatures (813 K in Fig. 1), autoignition looks like a two-stage process, although at 813 K and lower temperatures it actually takes place in three stages (multistage process), as evidenced by Fig. 2 for $T_0 = 813$ K. Here, the first stepwise temperature rise occurs at $t \sim 1.2$ ms; it is associated with the occurrence of cool flame. The occurrence of blue flame and hot explosion is observed after ~2.1 and ~2.7 ms, respectively. The sequential occurrence of cool and blue flames and hot explosion is the manifestation of the multistage pattern of autoignition. An acceleration of the reaction in cool flame is a consequence of branching induced by the decomposition of isomerized alkyl hydroperoxide $CH_3C(CH_3)_2CH_2CH(CH_3)CH_2O_2H$ to form hydroxyl and oxyradical. Blue flame is attributed to branching caused by the decomposition of hydrogen peroxide H_2O_2, as evidenced by the behavior of the calculated curves for peroxides and two hydroxyl concentration peaks. In experimental pressure records, the separation of stages may be not so pronounced

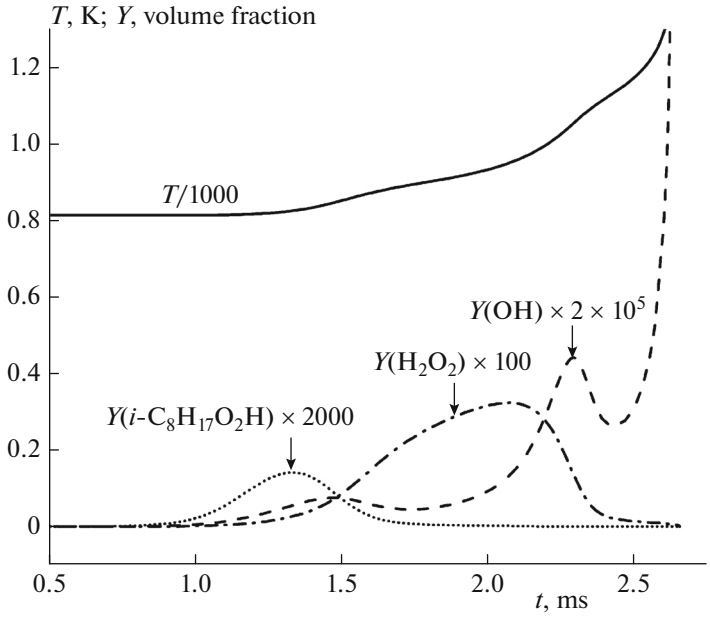

Fig. 2. Calculated time dependences of temperature T and volume fractions of hydroxyl and peroxides Y during the autoignition of a stoichiometric ($f = 1.0$) isooctane–air mixture at an initial pressure of $P = 36$ atm and an initial temperature of $T_0 = 813$ K.

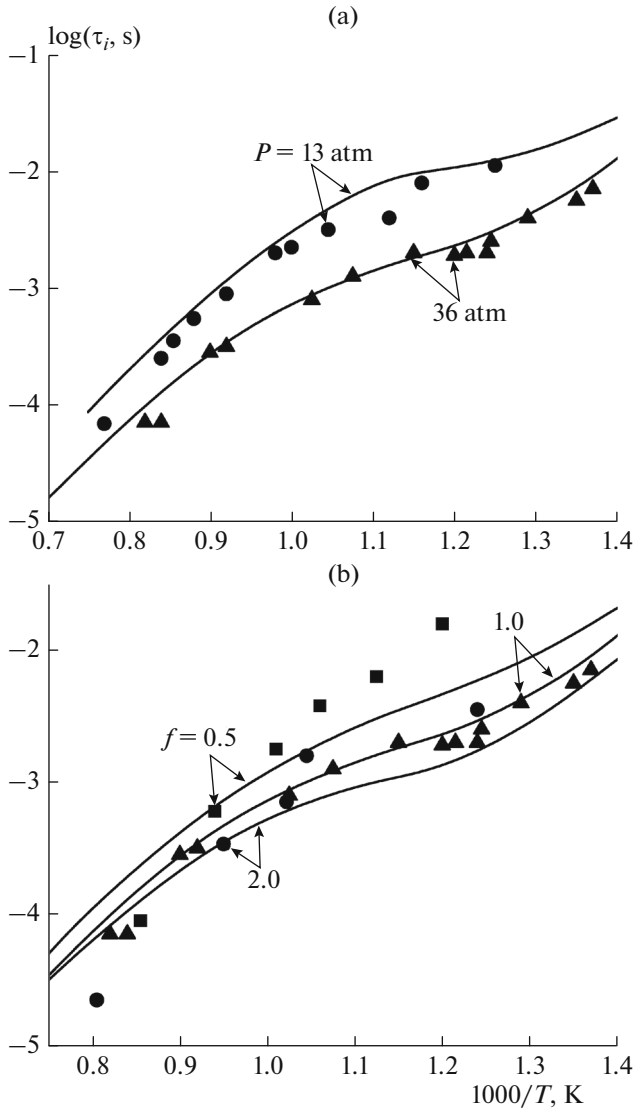

Fig. 3. Ignition delays of isooctane–air mixtures at different temperatures, pressures, and compositions: (a) $f = 1.0$, $P = 13$ and 36 atm and (b) $f = 0.5$, 1.0, and 2.0, $P = 36$ atm. The symbols correspond to the experimental data [10]; the curves denote the calculation.

because of temperature inhomogeneities in the reaction volume; however, in fact, it is locally implemented.

The calculation results were compared with the experimental data on the autoignition of isooctane described in the literature. Figure 3 shows ignition delays of isooctane–air mixtures at different temperatures for pressures of 13 and 36 atm. The symbols correspond to the experimental data [10]; the curves denote the calculation.

The occurrence of cool and blue flames during the oxidation and autoignition of isooctane was previously described in [11]. Experimental pressure records derived in [11] at an initial temperature of 643 K and different initial pressures are reproduced in Fig. 4. Figure 5 shows the calculation results for the same conditions with allowance for heat transfer, while disregarding the reactions on the reaction vessel walls; at these pressures and temperatures, these reactions can affect the chemical process; however, their simulation is hindered by the lack of kinetic data. The two figures show that, at initial pressures of $P = 0.8$–1.4 atm, isooctane undergoes oxidation in the presence only of cool flames, whereas at pressures of 2.3 (experiment) and 1.9 atm (calculation), multistage autoignition takes place.

Figure 6a shows the experimental time dependence (curve) of hydroxyl concentration for a 0.05% i-C_8H_{18} + 0.625% O_2 + Ar mixture, which was derived in [12] at $T_0 = 1511$ K and $P = 1.51$ atm; the respective calculated dependence plotted with the use of the developed DKM is shown in Fig. 6b.

Figure 7 shows the calculated temperature dependences of ignition delay for stoichiometric mixtures of n-pentane n-C_5H_{12}, isohexane $(CH_3)C_5H_{11}$, isoheptane $(CH_3)_2C_5H_{10}$, and isooctane $(CH_3)_3C_5H_9$ at a pressure of $P = 36$ atm. For comparison, the figure shows experimental points [10] for isooctane and n-heptane n-C_7H_{16} (symbols); in this case, the points for n-heptane correspond to a pressure of $P = 42$ atm. Comparison of the calculated and experimental data can generally be regarded as satisfactory.

Laminar Flame Propagation

Additional calculations were conducted to determine the laminar flame propagation velocity u_n in isooctane–air mixtures of varying composition. Calculations were conducted as described in [13]. Figure 8 shows comparison of the calculated u_n values with the experimental results of [14–17] at an initial temperature of $T_0 = 298$ K and atmospheric pressure.

Autoignition of Droplets

The developed DKM was also used to calculate the autoignition and combustion of liquid droplets. The calculation was based on unsteady-state one-dimensional (spherical symmetry) equations of conservation of mass, chemical components, and energy for the gas and condensed phases; the solutions were conjugated on the droplet surface. A detailed description of the mathematical model and calculation technique is given in [18]. It was assumed that the initial temperature of the air around the droplet T_{g0} is constant and the initial temperature of the liquid T_{l0} is always 293 K. The initial radius of the calculated region around the droplet R_0 was assumed to be much larger than initial droplet radius r_0. According to [18], any selected R_0 value corresponds to a certain value of equivalence ratio f in a uniform monodisperse droplet–gas suspen-

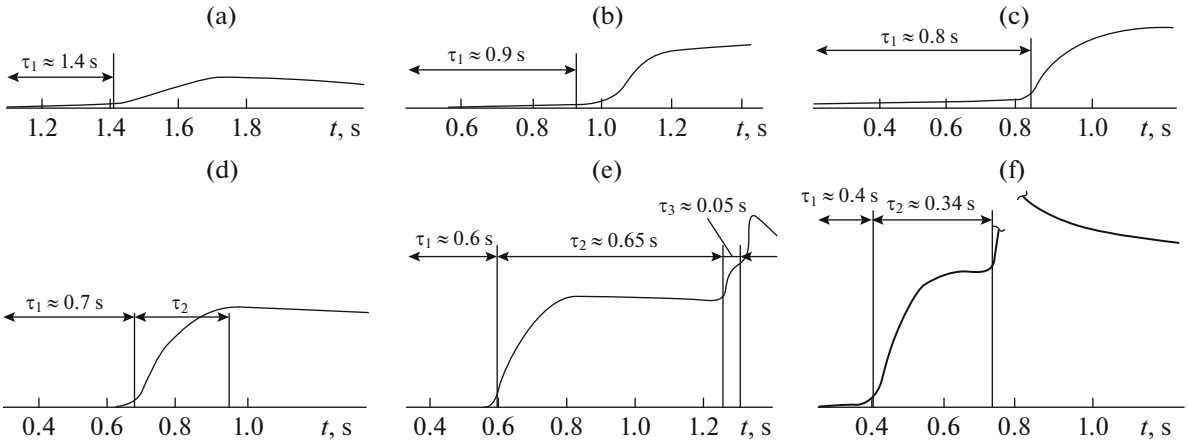

Fig. 4. Pressure records during the oxidation and autoignition of a rich isooctane–air mixture with $f = 1.25$ (excess air factor $\alpha = 0.8$) at $T_0 = 643$ K and different initial pressures: $P =$ (a) 0.8, (b) 1.05, (c) 1.4, (d) 1.8, (e) 2.3, and (f) 3.2 atm [11].

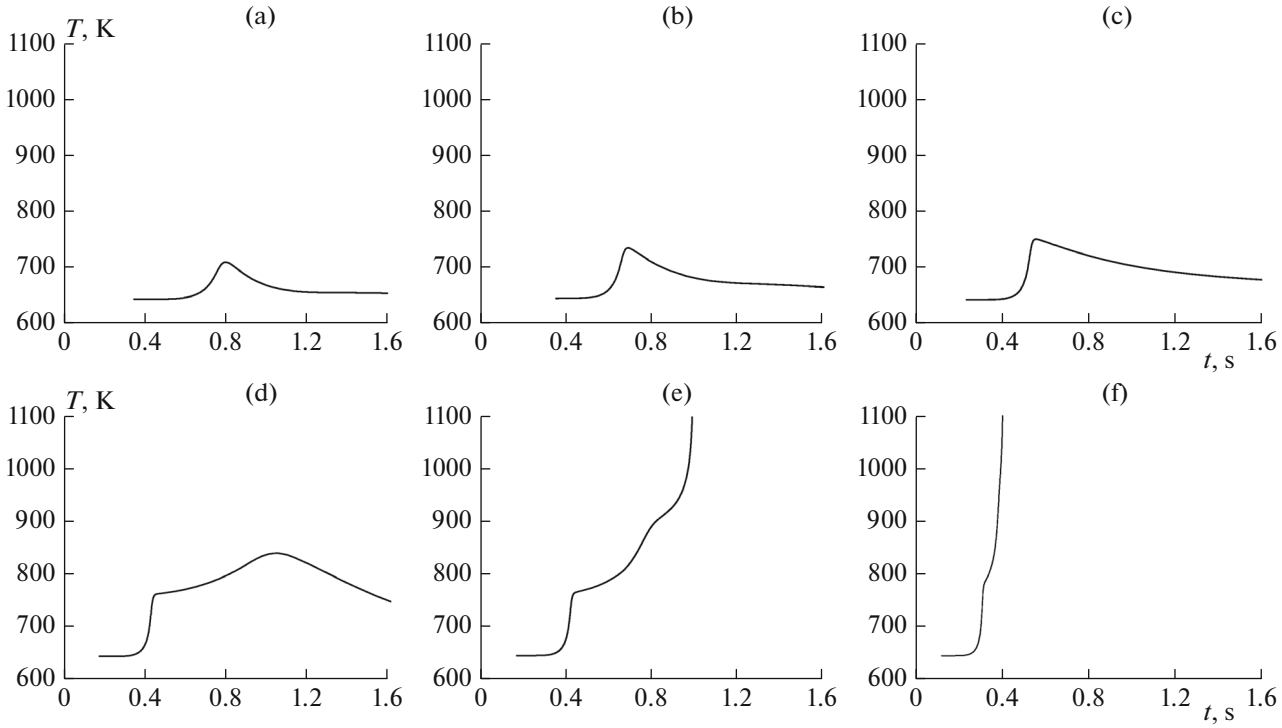

Fig. 5. Calculated temperature–time dependences during the oxidation and autoignition of a rich isooctane–air mixture with $f = 1.25$ (excess air factor $\alpha = 0.8$) at $T_0 = 643$ K and different initial pressures: $P =$ (a) 0.8, (b) 1.05, (c) 1.4, (d) 1.8, (e) 1.9, and (f) 3.2 atm.

sion. After a certain time—an autoignition induction period—autoignition occurred in the gas at a certain distance from the center of the droplet.

Figure 9 shows the calculation results for the autoignition of a single isooctane droplet in the air in the form of time dependences of maximum gas temperature $T_{g,max}$ and squared droplet diameter d^2 at an initial air temperature of $T_{g0} = 1220$ K and an initial pressure of $P = 1$ atm. Calculation was conducted for a droplet with an initial diameter of $d_0 = 2r_0 = 300$ μm. It is evident that the squared droplet diameter initially increases and then (as the $T_{g,max}(t)$ curve begins to ascend) stepwise decreases; after some time, the $d^2(t)$ curve acquires an almost constant (negative) slope. The initial increase in the droplet size is attributed to the thermal expansion of the liquid during heating. The behavior of the $d^2(t)$ curve in the final—almost

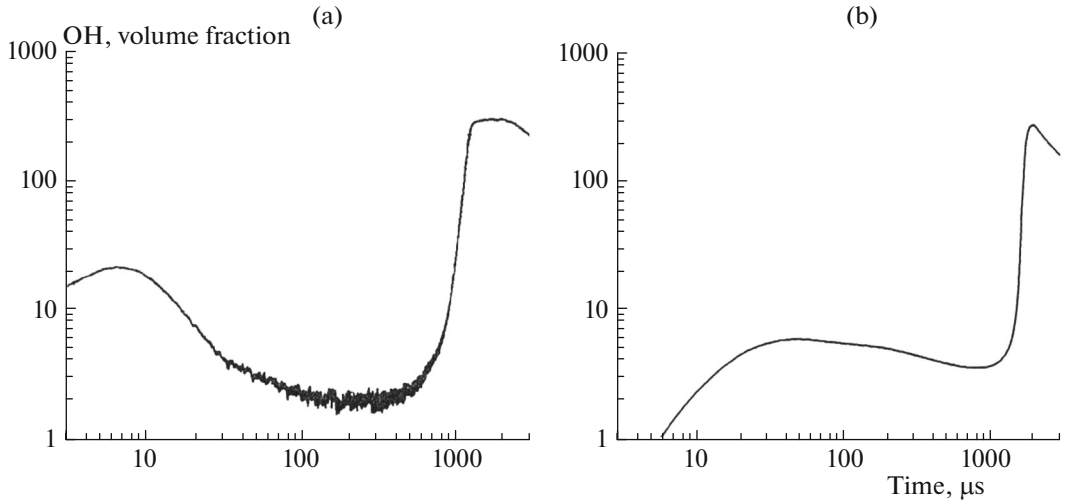

Fig. 6. Time dependences of the hydroxyl concentration (in ppm) during the autoignition of a 0.05% i-C_8H_{18} + 0.625% O_2 + Ar mixture at T_0 = 1511 K and P = 1.51 atm: (a) experimental data [12] (thick line) and (b) calculation.

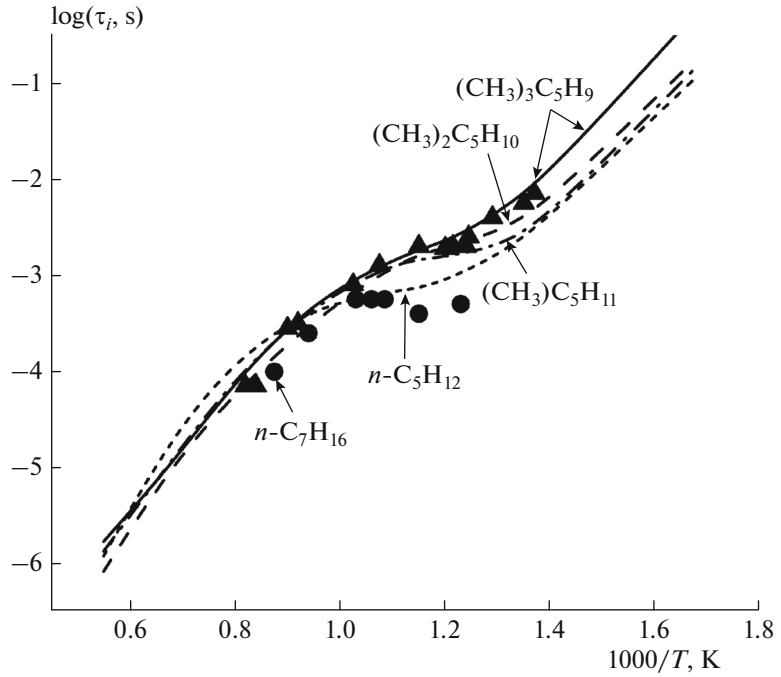

Fig. 7. Comparison of the calculated ignition delays of stoichiometric mixtures of n-pentane, isohexane, isoheptane, and isooctane with air (curves) with the measured values for isooctane and n-heptane (symbols [10]).

linear—portion can provide information about droplet combustion rate constant k; in this case, k = 0.00797 cm^2/s. This result agrees with the experimental k values obtained in [19] for large isooctane droplets.

Figure 10 shows comparison of the calculated (curve) and measured (circles [20]) dependences of ignition delay τ_i of individual isooctane droplets in the air on initial droplet diameter d_0 at T_{g0} = 1220 K and P = 1 atm. The agreement between the results can be considered satisfactory.

Compression-Induced Autoignition under Conditions of an Internal Combustion Engine (ICE)

An important aspect in the study of hydrocarbons is the properties exhibited by these materials during compression-induced autoignition under conditions of an ICE, i.e., their antiknock propensity. The currently available programs [21, 22] make it possible to approximately calculate the basic characteristic of the antiknock propensity of hydrocarbons—their tendency to autoignition. To determine the tendency to

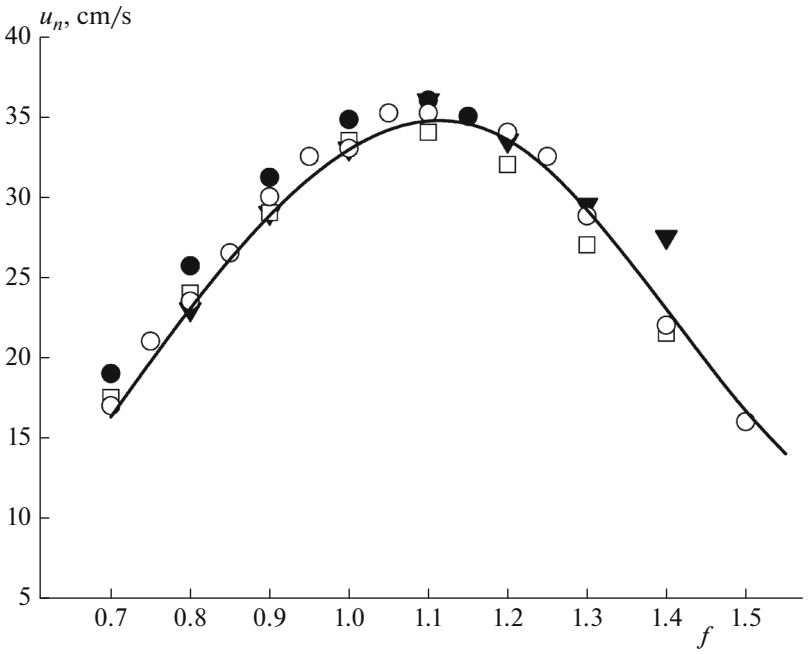

Fig. 8. Dependences of laminar flame propagation velocity u_n in isooctane–air mixtures on equivalence ratio f (atmospheric pressure, $T_0 = 298$ K): (filled circle) [14], (open square) [15], (open circle) [16], and (filled inverted triangle) [17]; the curve denotes calculation.

autoignition, it is necessary to construct the so-called indicator diagram, which represents the dependence of the pressure in the engine cylinder on the crank angle (CA) during piston motion. Figure 11 shows an example of the calculated indicator diagram for the autoignition of a fuel–air mixture. Calculation was conducted without taking into account the heat transfer of the gases with the ICE cylinder walls. Compression of a homogeneous fuel–air mixture begins when the piston is located at bottom dead center (BDC, –180 CA degrees (CAD)) and the cylinder volume achieves a maximum value and ends at the top dead center (TDC, 0 CAD) when the cylinder volume achieves a minimum value. In this example, at an

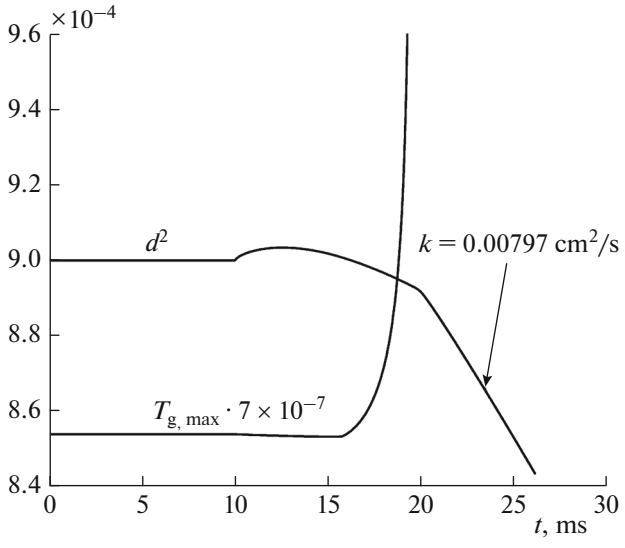

Fig. 9. Calculated time dependences of maximum gas temperature $T_{g,max}$ [K] and squared isooctane droplet diameter d^2 [cm^2] during the autoignition of the droplet at $d_0 = 300$ μm, $T_{g0} = 1220$ K, and $P = 1$ atm.

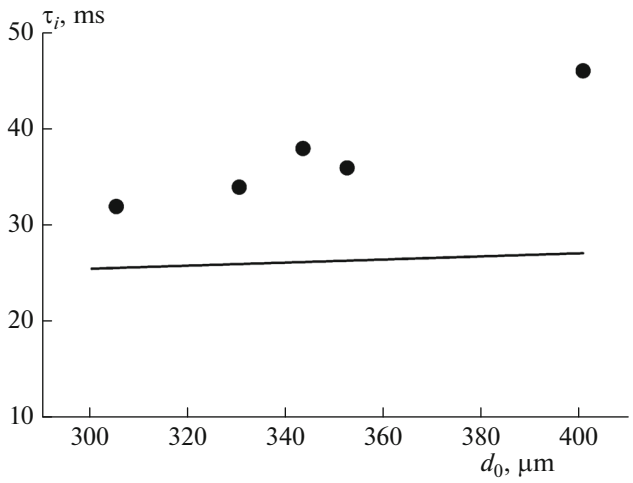

Fig. 10. Comparison of the calculated (curve) and measured dependences (circles [20]) of autoignition induction period τ_i on initial isooctane droplet diameter d_0 at $T_{g0} = 1220$ K and $P = 1$ atm.

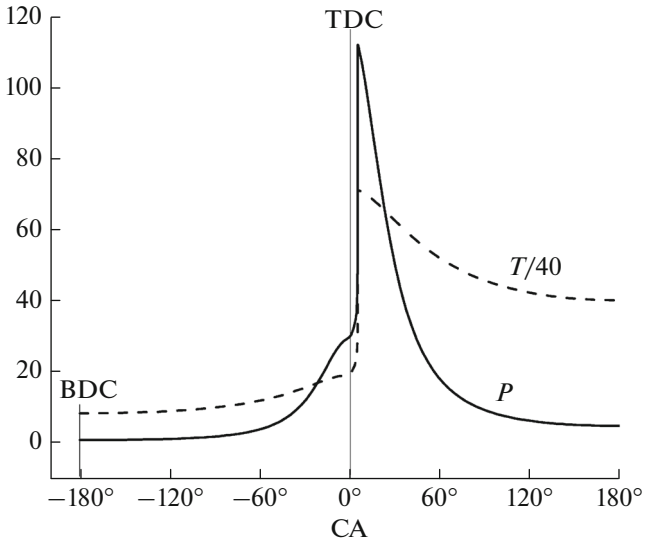

Fig. 11. Calculated dependences of pressure P [atm] and temperature T [K] on time (in terms of CA) for a stoichiometric i-C_8H_{18}–air mixture in an ICE at an initial pressure of $P = 1$ atm, an initial temperature of $T_0 = 340$ K, a compression ratio of $\varepsilon = 13$, and an ICE shaft speed of $n = 600$ min^{-1}.

engine shaft speed of $n = 600$ min^{-1}, the compression time is $t = 0.05$ s (1 CAD corresponds to a time of ~0.278 ms) and the compression ratio is $\varepsilon = 13$ (maximum to minimum cylinder volume ratio). Figure 11 characterizes the autoignition of the mixture that begins at the TDC and the combustion of the mixture during expansion (maximum pressure and temperature is achieved at ~5 CAD).

Figure 12 shows the calculated dependences of the gas temperature in an ICE cylinder on CA for stoichiometric air mixtures of normal pentane n-C_5H_{12}, isohexane i-C_6H_{14}, isoheptane i-C_7H_{16}, and isooctane i-C_8H_{18}, which are hydrocarbons that have a linear five-membered chain with the same number of carbon atoms. It is evident from Fig. 12 that, in this series of hydrocarbons, the antiknock properties increase from left to right. In actual practice, the antiknock propensity of fuels is determined by a special technique in terms of the so-called octane number (ON): the higher the ON, the longer the ignition delay. According to reference data, the ON of n-C_5H_{12}, i-C_6H_{14} ($(CH_3)C_5H_{11}$), i-C_7H_{16} ($(CH_3)_2C_5H_{10}$), and i-C_8H_{18} ($(CH_3)_3C_5H_9$) is 61, 73, 85, and 100, respectively. Thus, the calculated data in Fig. 12 qualitatively agree with the experiment. This conclusion holds true for the mutual arrangement of the calculated lines and the experimental points in Fig. 7.

The results suggest that the developed DKM provides a qualitatively correct description of the kinetic behavior of paraffin hydrocarbon fuels in the entire range of ON (0 to 100) while varying the content of n-heptane n-C_7H_{16} (ON = 0) and isooctane i-C_8H_{18} (ON = 100) in a binary mixture. Figure 13 shows the temperature dependences of ignition delays for these binary mixtures with different ONs.

CONCLUSIONS

A DKM of oxidation and combustion of isooctane has been proposed. The mechanism includes the main

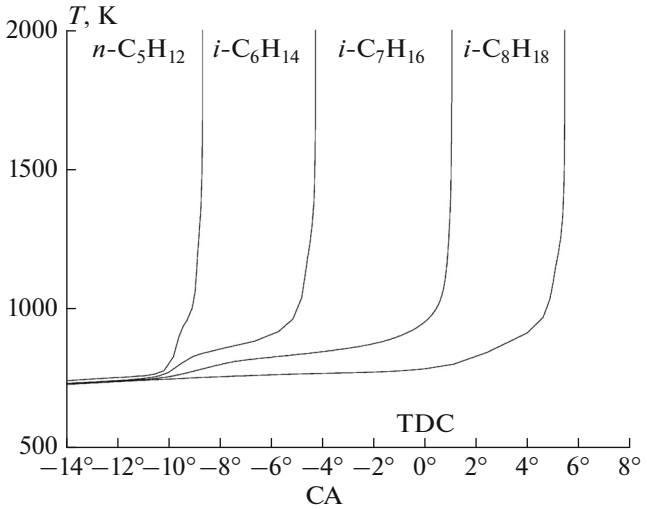

Fig. 12. Dependence of temperature T on time (in terms of CA) for stoichiometric mixtures of n-C_5H_{12}, i-C_6H_{14}, i-C_7H_{16}, and i-C_8H_{18} with air at a compression ratio of $\varepsilon = 13$, $P = 1$ atm, $T_0 = 340$ K, and $n = 600$ min^{-1}.

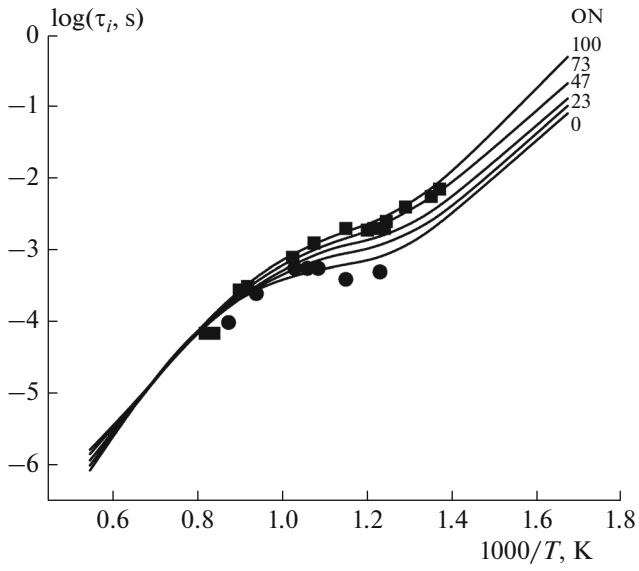

Fig. 13. Comparison of the calculated (curves) and measured ignition delays (squares, isooctane; circles, n-heptane [13]) of stoichiometric n-heptane–isooctane–air mixtures at different ON and $P = 36$ atm and at ON = 0 (pure n-heptane) and $P = 42$ atm.

processes that determine the reaction rate and the formation of the main intermediates and end products and has the status of an ab initio detailed mechanism because all the constituent elementary reactions have a kinetic substantiation. The mechanism is based on a nonextensive approach in which the key point is the generality of the main process pathways and the major types of elementary events, rather than the variety of products and reactions. To switch from the detailed mechanism of oxidation of isobutane to the oxidation of isooctane, the following simplifications were introduced: (1) schemes with the so-called double addition of oxygen (first, to the peroxy radical and then to the isomerized form thereof) were not used because the first addition was considered sufficient and (2) the variety of products and reactions was limited; however, the main process pathways and the key types of elementary events were preserved.

The developed DKM of oxidation of isooctane is fairly compact (kinetic mechanism data file will be posted on the website www.combex.ru). The most important feature of the mechanism is the manifestation of a multistage pattern in the form of occurrence of cool and blue flames in the case of low-temperature autoignition. Characteristics of the autoignition and combustion of homogeneous mixtures and liquid droplets with the air in a wide range of initial conditions have been calculated; comparison of the calculation results with the experimental data has yielded their satisfactory agreement. The findings suggest that the adopted approach to the construction of the mechanism and the selection of the main reaction pathways are apparently correct.

ACKNOWLEDGMENTS

This work was partially supported by the Ministry of Education and Science of the Russian Federation under state contract no. 14.609.21.0001 (contract identifier RFMEFI57914X0038) "Development of a Technology for the Generation of Hydrojet Thrust in Hydrojet Engines of High-Speed Waterborne Crafts and the Preparation of a Bench Display Sample of a Hydrojet Pulse Detonation Engine" in the framework of the federal target program "Research and Development in Priority Fields of Science and Engineering in Russia for 2014–2020."

REFERENCES

1. A. S. Sokolik, *Self-Ignition, Flame and Detonation in Gases* (Akad. Nauk SSSR, Moscow, 1960) [in Russian].
2. D. Downs, J. S. Street, and R. W. Wheeler, Fuel **32**, 279 (1953).
3. C. K. Westbrook, J. Warnatz, and W. J. Pitz, Proc. Combust. Inst. **22**, 893 (1988).
4. E. Ranzi, T. Faravelli, P. Gaffuri, et al., Combust. Flame 108, 24 (1997).
5. H. Machrafi and S. Cavadias, Combust. Flame **155**, 557 (2008).
6. V. Ya. Basevich, A. A. Belyaev, V. S. Posvyanskii, and S. M. Frolov, Russ. J. Phys. Chem. B **7**, 161 (2013).
7. V. Ya. Basevich, A. A. Belyaev, S. N. Medvedev, V. S. Posvyanskii, and S. M. Frolov, Russ. J. Phys. Chem. B **9**, 268 (2015).
8. V. Ya. Basevich, A. A. Belyaev, S. N. Medvedev, V. S. Posvyanskii, and S. M. Frolov, Russ. J. Phys. Chem. B **9**, 933 (2015).
9. R. C. Reid, J. M. Prausnitz, and T. K. Sherwood, *The Properties of Gases and Liquids* (McGraw-Hill, New York, 1977).
10. K. Fieweger, R. Blumenthal, and G. Adomeit, Proc. Combust. Inst. **25**, 1579 (1994).
11. A. S. Sokolik and S. A. Yantovskii, Zh. Fiz. Khim. **20**, 13 (1946).
12. M. A. Oehlschlaeger, D. F. Davidson, J. T. Herbon, and R. K. Hanson, Int. J. Chem. Kinet. **36**, 67 (2004).
13. A. A. Belyaev and V. S. Posvyanskii, Algoritmy Programmy. Inform. Byull. Gos. Fonda Algoritmov Programm SSSR, No. 3, 35 (1985).
14. E. H. Nilsson, *Combustion Kinetics of Liquid Fuels* (Lund Univ., Lund, Sweden, 2010), p. 94.
15. Y. Huang, C. J. Sung, and J. A. Eng, Combust. Flame **139**, 239 (2004).
16. S. G. Davis and C. K. Law, Proc. Combust. Inst. **27**, 521 (1998).
17. K. Kumar, J. E. Freeh, C. J. Sung, and Y. Huang, J. Propuls. Power **23**, 428 (2007).
18. V. Ya. Basevich, A. A. Belyaev, S. N. Medvedev, V. S. Posvyanskii, F. S. Frolov, and S. M. Frolov, Russ. J. Phys. Chem. B **4**, 995 (2010).
19. G. A. E. Godsave, Proc. Combust. Inst. **4**, 819 (1953).
20. J.-R. Yang, C.-Y. Yukao, J.-J. Whang, and S.-C. Wong, Combust. Flame **123**, 266 (2000).
21. V. Ya. Basevich, A. A. Belyaev, A. N. Gots, V. S. Posvyanskii, I. V. Semenov, S. M. Frolov, and F. S. Frolov, in *Combustion and Explosion,* Ed. by S. M. Frolov (Torus Press, Moscow, 2012), **5**, 167 [in Russian].
22. CHEMKIN-PRO Release 15083 (2009).

Translated by M. Timoshinina